North American Monsoon and Associated Intraseasonal Variability Simulated by IPCC AR4 Coupled GCMs

Jia-Lin Lin[1], Brian E. Mapes[2], Klaus M. Weickmann[1], George N. Kiladis[1], Siegfried D. Schubert[3], Max J. Suarez[3], Julio T. Bacmeister[3], and Myong-In Lee[3]

[1]NOAA ESRL/CIRES Climate Diagnostics Center, Boulder, CO
[2]RSMAS, University of Miami, Miami, FL
[3]NASA GSFC Global Modeling and Assimilation Office, Greenbelt, MD

Submitted to *J. Climate*
November 2006

Corresponding author address: Dr. Jia-Lin Lin
NOAA ESRL/CIRES Climate Diagnostics Center
325 Broadway, R/PSD1, Boulder, CO 80305-3328
Email: jialin.lin@noaa.gov

Abstract

This study evaluates the fidelity of North American monsoon and associated intraseasonal variability in IPCC AR4 (the Inter-governmental Panel on Climate Change Fourth Assessment Report) coupled general circulation models (GCMs). Twenty years of monthly precipitation from each of the 22 models' 20th century climate simulation, together with the available daily precipitation from 14 of them, are analyzed and compared with GPCP monthly and daily precipitation. We focus on the seasonal cycle and horizontal pattern of monsoon precipitation, together with the two dominant intraseasonal modes: the eastward-propagating Madden-Julian oscillation (MJO) and the westward-propagating easterly waves.

The results show that current state-of-the-art GCMs have significant problems and display a wide range of skill in simulating the North American monsoon and associated intraseasonal variability. Most of the models reproduce the monsoon rain belt extending from southeast to northwest. However, most models overestimate the precipitation over the core monsoon region throughout the seasonal cycle. Although many models reproduce the gradual northward shift of precipitation from March to July, several models simulate a nearly simultaneous increase of precipitation in northern and southern latitudes, leading to a too-early monsoon onset. Moreover, most models fail to reproduce the gradual southward shift of precipitation from August to November, and keep the high precipitation in monsoon region until the end of the year.

Regarding the intraseasonal modes, most of the models produce overly weak variances for both the MJO and easterly waves, and simulate poor eastward propagation

of the MJO. Nevertheless, most models simulate good westward propagation of the easterly waves.

1. Introduction

The North American monsoon, variously known as the Southwest United States monsoon, the Mexican monsoon, or the Arizona monsoon, significantly affects the precipitation and large-scale circulation over much of the western United States and northwestern Mexico (e.g. Douglas et al. 1993; Higgins et al. 1997; Adams and Comrie 1997; Barlow et al. 1998; Vera et al. 2006; see schematic in Figure 1), which stimulated strong interest of the prediction and research communities, leading to the recent North American Monsoon Experiment (NAME; Higgins et al. 2003, 2006). The North American monsoon also has strong intraseasonal variability with two dominant modes: the Madden-Julian Oscillation (MJO) that propagates eastward from the western and central Pacific (e.g. Higgins and Shi 2001; Lorenz and Hartmann 2006), and easterly waves that propagate westward from the Atlantic Ocean (e.g. Lau and Lau 1990; Avila 1991; Avila and Pasch 1992; Molinari et al. 1997; Raymond et al. 1998; Zehnder et al. 1999; Molinari et al. 2000; Fuller and Stensrud 2000; Serra and Houze 2002; Peterson et al. 2003), both of which significantly modulate the monsoon precipitation, and the formation, intensity and track of the tropical cyclones. Therefore, they are important for both weather and climate prediction.

Many previous studies have used high-resolution regional models to simulate the North American monsoon and associated intraseasonal variability, and there have been significant improvements from earlier simulations to recent studies (e.g. Giorgi 1991; Giorgi et al. 1994; Dunn and Horel 1994a, b, Stensrud et al. 1995; Anderson et al. 2000a, b, 2001, Anderson 2002; Anderson and Roads 2002; Xu and Small 2002; Gochis et al. 2002, 2003; Mo and Juang 2003; Kanamitsu and Mo 2003; Saleeby and Cotton 2004;

Liang et al. 2004; Xu et al. 2004; Li et al. 2004, 2005). Currently there is a comprehensive multi-model intercomparison project associated with the NAME experiment (Gutzler et al. 2005). For the general circulation models (GCMs), on the other hand, only several previous studies have examined the simulations of the North American monsoon and associated intraseasonal variability by *individual* models (e.g. Krishnamurti et al. 2000; Arritt et al. 2000; Yang et al. 2001; Berbery and Fox-Rabinovitz 2003; Kunkel 2003; Farrara and Yu 2003; Collier and Zhang 2006). The success of these simulations is sensitive to a variety of factors, such as horizontal resolution (Berbery and Fox-Rabinovitz 2003), boundary conditions (Yang et al. 2001), and convective parameterization (Collier and Zhang 2006). However, to our knowledge, no multi-model intercomparison has been conducted to evaluate the general status of the simulations of North American monsoon and associated intraseasonal variability in the state-of-the-art GCMs.

Recently, in preparation for the Inter-governmental Panel on Climate Change (IPCC) Fourth Assessment Report (AR4), more than 20 international climate modeling centers conducted a comprehensive set of long-term simulations for both the 20th century's climate and different climate change scenarios in the 21st century. Before conducting the extended simulations, many of the modeling centers overhauled their physical schemes to incorporate the state-of-the-art research results. Many model-intercomparison studies have evaluated the dominant tropical modes simulated by the IPCC AR4 coupled GCMs, such as the time-mean ITCZ (e.g. Lin 2006), ENSO (e.g. AchutaRao and Sperber 2006; Capotondi et al. 2006; Joseph and Nigam 2006), the MJO and convectively coupled equatorial waves (Lin et al. 2006). For example, Lin et al. (2006) evaluated the all-season

behavior of MJO and convectively coupled equatorial waves in 14 IPCC AR4 models. They found that most of the state-of-the-art coupled GCMs simulate too-weak MJO variance and poor MJO propagation, as well as too-weak variances and too-fast phase speeds for other convectively coupled equatorial waves. However, no previous study has evaluated the North American monsoon or its associated intraseasonal variability in the IPCC AR4 models.

The purpose of this study is to evaluate the North American monsoon and associated intraseasonal variability in IPCC AR4 coupled GCMs. To our knowledge, this is the first GCM intercomparison in the literature for the North American monsoon and associated intraseasonal variability. The questions we address are:

(1) How well do the IPCC AR4 models simulate the North American monsoon?

(2) How well do the IPCC AR4 models simulate the intraseasonal precipitation signals associated with the North American monsoon, especially the MJO and tropical easterly waves?

(3) Is there any systematic dependence of model simulations on the basic characteristics of convection schemes, such as their closure assumptions, or model resolution?

The models and validation datasets used in this study are described in section 2. The diagnostic methods are described in section 3. Results are presented in section 4. A summary and discussion are given in section 5.

2. Models and validation datasets

This analysis is based on 21 years (model year 1979-1999) of the Climate of the 20th Century (20C3M) simulations from 22 IPCC AR4 coupled GCMs. Table 1 shows the model names and acronyms, their horizontal and vertical resolutions, and brief descriptions of their deep convection schemes. For each model we use twenty years of monthly mean surface precipitation. In addition, daily precipitation is available for 14 of the models, and we use eight years of daily data from each model to study the intraseasonal variability.

The model simulations are validated using the Global Precipitation Climatology Project (GPCP) Version 2 Precipitation (Adler et al. 2003; Huffman et al. 2001). We use 21 years (1979-1999) of monthly data with a horizontal resolution of 2.5 degree longitude by 2.5 degree latitude, and eight years (1997-2004) of daily data with a horizontal resolution of 1 degree longitude by 1 degree latitude.

3. Method

The MJO is defined as significant rainfall variability in eastward zonal wavenumbers 1-6 and in the period range of 24-70 days. It is isolated using the following procedure: (1) The 8 years of daily precipitation data was averaged along the latitude belt between 5N and 25N, where the eastward propagation of MJO mainly occurs during northern summer, with a zonal resolution of 10 degrees longitude. (2) The space-time spectrum was calculated using discrete Fourier transform for the whole 8-year time series. (3) Then we used an inverse space-time Fourier transform to get the time series of the eastward wavenumbers 1-6 component, which includes all available frequencies. (4) Then these

time series were filtered using a 365-point 24-70 day Lanczos filter (Duchan 1979), whose response function is shown in Figure 4. Because the Lanczos filter is non-recursive, 182 days of data were lost at each end of the time series (364 days in total). (5) The resultant eastward wavenumbers 1 through 6, 24-70 day anomaly during northern summer (May-October) is hereafter referred to as the MJO anomaly. (6) Its variance was also compared with the variance of its westward counterpart, i.e., the westward wavenumbers 1-6, 24-70 day anomaly, which was isolated using the same method as above.

The procedure for isolating the westward-propagating easterly waves is also same as above except for the westward wavenumber 6 and up, 3-6 day mode (e.g. Kiladis et al. 2006). Its variance was also compared with the variance of its eastward-propagating counterpart, i.e., the eastward wavenumber 6 and up, 3-6 day anomaly, which was isolated using the same method as above.

4. Results

a Seasonal variation of precipitation

Figure 2a shows the seasonal cycle of precipitation averaged over the core region of North American monsoon between 20N-32.5N and 245E-260E for observations and 22 IPCC AR4 coupled GCMs. Figure 2a demonstrates three points. First, the IPCC AR4 models display a large scatter in precipitation amplitude with most of the models producing excessive precipitation throughout the whole seasonal cycle. Second, in observations the monsoon onset is in July, but the models display a wide range of onset time with many models having a June onset (e.g. PCM, BCCR, CCSM3, MIROC-hires).

Third, in observations the monsoon ends in October, but many models keep the high monsoon precipitation until the end of the year (e.g. CNRM, PCM, IPSL, GISS-ER, BCCR, CCSM3).

Figure 2b is same as Figure 2a but for the eastern Pacific warm pool region between 10N-20N and 245E-260E. In contrast to the excessive precipitation over the core region of North American monsoon, many models produce insufficient precipitation over the eastern Pacific warm pool. The observed monsoon onset time is June in this region, which is reproduced by many models. However, the observed ending of the monsoon in October is not well reproduced by many models, which tend to keep high precipitation until the end of the year.

To examine the northward/southward shift of monsoon precipitation, Figure 3 shows the seasonal cycle of precipitation along the longitude belt between 245E-260E. In observations (Figure 3a, repeated in Figure 3b), the precipitation displays a gradual northward shift from March to July, and a gradual southward shift from August to November. The model simulations show two characteristics. First, although many models can reproduce the gradual northward shift (e.g. CGCM-T47, IAP, GISS-AOM, HadCM3, GFDL2.0, MPI), there are quite a few models which produce a (nearly) simultaneous increase of precipitation in northern and southern latitudes in early summer (e.g. PCM, GISS-ER, GFDL2.1, CNRM, BCCR), leading to the too-early monsoon onset in those models over the core region of North American monsoon (Figure 2a). Second, most of the models fail to reproduce the gradual southward shift of precipitation from August to November, and keep high precipitation in the northern latitudes until the end of the year.

Next we look at the horizontal pattern of precipitation in July when the monsoon is at its peak (Figure 4). The observed precipitation (Figure 4a, repeated in Figure 4b) displays a rain belt extending from southeast to northwest. Most of the models produce the rain belt, suggesting that the models can capture the basic mechanism for the formation of North American monsoon, although the magnitude is often too large. In addition, in several models the simulated rain belt is isolated from the precipitation over eastern Pacific warm pool, which is different from observations (e.g. CSIRO, MIROC-medres, MIROC-hires).

In summary, most of the IPCC AR4 coupled GCMs reproduce the monsoon rain belt extending from northwest to southeast over Arizona and north Mexico. However, most of the models overestimate the precipitation over the core monsoon region throughout the seasonal cycle. Although many models reproduce the gradual northward shift of precipitation from March to July, several models simulate a nearly simultaneous increase of precipitation in northern and southern latitudes, leading to a too-early monsoon onset. Most of the models fail to reproduce the gradual southward shift of precipitation from August to November, and keep the high precipitation in monsoon region until the end of the year.

b The MJO

Now we focus on the variance of the MJO, i.e., the daily variance of the eastward wavenumbers 1-6, 24-70 day mode. Figure 5 shows the MJO variance along the equator averaged between 5N and 25N. In observations, MJO variance has its maximum over the eastern Pacific warm pool. The model variance approaches the observed value in only one model (ECHAM5/MPI-OM), but is less than half of the observed value in all other

13 models. This is similar to the performance of the IPCC AR4 models in simulating the all-season MJO over the Indian Ocean and western Pacific, for which the simulated variance is less than half of the observed value in 12 of the 14 models.

In addition to the variance, another important index for evaluating the MJO simulation is the ratio between the variance of the eastward MJO and that of its westward counterpart, i.e., the westward wavenumbers 1-6, 24-70 day mode, which is important for the zonal propagation of tropical intraseasonal oscillation. Figure 6 shows the ratio between the eastward variance and the westward variance averaged over an eastern Pacific box between 5N-25N and 220E-260E. In observation, the eastward MJO variance is double that of the westward variance. Of the 14 models, four models simulate a ratio larger than 1.5 (GFDL2.0, GFDL2.1, MIROC-hires, and CSIRO), but all other 10 models produce a too small ratio that is close to one, or even less than one (i.e., westward variance dominates over eastward variance).

The competition between the eastward MJO variance and its westward counterpart largely determines the zonal propagation characteristics of the tropical intraseasonal oscillation. A useful method for evaluating the MJO simulation is to look at the propagation of 30-70 day filtered anomaly of the raw precipitation data, which includes all wavenumbers, to see if the MJO mode (the eastward wavenumber 1-6 mode) dominates over other modes, as is the case in observations. Because the tropical intraseasonal oscillation is dominated by zonally asymmetric, planetary-scale phenomena, the competition is mainly between the MJO and its westward counterpart - the westward wavenumber 1-6 component. Figure 7 shows the lag-correlation of 30-70 day precipitation anomaly averaged between 5N and 25N with respect to itself at

10N255E. The observational data shows prominent eastward propagating signals of the MJO, with a phase speed of about 5 m/s. The models display a wide range of propagation characteristics that are consistent with the ratio between the eastward MJO variance and its westward counter part shown in Figure 6. The four models with a realistic or too large ratio (GFDL2.0, GFDL2.1, MIROC-hires, and CSIRO) show a discernable eastward propagating signal, but other models with the eastward/westward ratio being nearly equal to one or less than one show a standing oscillation (e.g. PCM, MRI) or westward propagation (e.g. GISS-AOM, GISS-ER).

To summarize, the model MJO variance is generally too small and is less than half of the observed value in 13 of the 14 models. The ratio between the eastward MJO variance and the variance of its westward counterpart is too small in most of the models, which is consistent with the lack of highly coherent eastward propagation of the MJO in many models.

c Easterly waves

Figure 8 shows the variance of easterly waves averaged between 10N-20N. Two of the 14 models (MPI and CNRM) simulate nearly realistic or overly large variance of easterly waves, but all other 12 models produce variance that is less than half of the observed value.

Figure 9 shows the ratio between the variance of the westward-propagating easterly waves and that of its eastward-propagating counterpart averaged over an eastern Pacific box between 10N-20N and 240E-290E. In observation, the westward variance roughly doubles the eastward variance. All models simulate a ratio larger than one (i.e., westward variance dominates over eastward variance), and three of the models simulate an overly

large ratio (MRI, MPI, and CNRM). Consistently, most of the models display a highly coherent westward propagation of easterly waves (not shown).

In short, the variance of easterly waves is close to or larger than the observed value in only two models, but is less than half of the observed value in all other 12 models. The ratio between the variance of westward-propagating easterly waves and that of its eastward-propagating counterpart is larger than one in all the models and overly large in three of the models, which is consistent with the highly coherent westward propagation of the easterly waves in most of the models.

5. Summary and discussion

This study evaluates the fidelity of North American monsoon and associated intraseasonal variability in IPCC AR4 coupled GCMs. Twenty years of monthly precipitation from each of the 22 models' 20th century climate simulation, together with the available daily precipitation from 14 of them, are analyzed and compared with GPCP monthly and daily precipitation. We focus on the seasonal cycle and horizontal pattern of monsoon precipitation, together with the two dominant intraseasonal modes: the eastward-propagating MJO and the westward-propagating easterly waves.

The results show that current state-of-the-art GCMs have significant problems and display a wide range of skill in simulating the North American monsoon and associated intraseasonal variability. Most of the models reproduce the monsoon rain belt extending from southeast to northwest. However, most models overestimate the precipitation over the core monsoon region throughout the seasonal cycle. Although many models reproduce the gradual northward shift of precipitation from March to July, several models

simulate a nearly simultaneous increase of precipitation in northern and southern latitudes, leading to a too-early monsoon onset. Moreover, most models fail to reproduce the gradual southward shift of precipitation from August to November, and keep the high precipitation in monsoon region until the end of the year.

Regarding the intraseasonal modes, most of the models produce overly weak variances for both the MJO and easterly waves, and simulate poor eastward propagation of the MJO. Nevertheless, most models simulate good westward propagation of the easterly waves.

Factors hypothesized to be important for simulating North American monsoon and associated intraseasonal variability include atmospheric model resolution, atmospheric model physics, and ocean model characteristics. We have three pairs of models with similar atmospheric models but in different resolution: CCSM3 (T85) vs PCM (T42), CGCM-T47 vs CGCM-T63, and MIROC-hires (T106) vs MIROC-medres (T42). CCSM3 does show better seasonal cycle and horizontal pattern than PCM (Figure 2a, Figure 3c,d, Figure 4c,d), but CGCM-T63 does not show significant improvement comparing with CGCM-T47 (Figure 2a, Figure 3e,f, Figure 4e,f), nor does MIROC-hires comparing with MIROC-medres (Figure 2a, Figure 3o,p, Figure 4o,p). Therefore, increasing atmospheric model resolution does not always improve the simulation of North American monsoon. For the intraseasonal variability, only one pair of the above models (MIROC-hires and MIROC-medres) has daily data available, and model higher resolution does not increase the variances of MJO (Figure 5) or easterly waves (Figure 8), although it does slightly improve the propagation of both the MJO (Figure 6) and easterly waves (Figure 9).

Regarding model physics, the 22 models provide a large variety of model physics, such as all the major deep convection schemes with different types of convective closures, convective triggers, and cloud models (Table 1). Models with same or similar deep convection schemes are listed together in Table 1 and in all the figures in this paper. For the seasonal cycle and horizontal pattern of North American monsoon, we do not find any systematic dependence of model simulations on the type of closure assumptions or cloud models. For the intraseasonal variability, however, the two models with the largest variances of easterly waves (MPI and CNRM; Figure 8) are the only models with their convective closure/trigger linked in some way to moisture convergence. The MPI model also produces the largest northern summer MJO variance in the North American monsoon region (Figure 5), and in addition, these two models simulate the largest all-season MJO variances over Indian Ocean and western Pacific (Lin et al. 2006). Therefore, moisture convergence closure/trigger seems to be helpful for improving MJO and easterly waves in GCMs.

Ocean model also plays some role in simulating the North American monsoon. Evidence comes from comparison between GISS-ER and GISS-EH, which have the same atmospheric model but different ocean models. GISS-EH produces somehow better seasonal cycle (Figure 3i, j) and horizontal pattern (Figure 4i, j).

It is important to note that the North American monsoon system is not an isolated system but is strongly affected by the whole tropical mean climate. Previous studies have shown that significant biases in tropical mean climate, especially the well-known double-ITCZ problem, exist in the IPCC AR4 models (e.g. Lin 2006). Therefore, improving the

simulation of the whole tropical mean climate may be a prerequisite for improving the simulation of North American monsoon.

Acknowledgements

Gary Russell kindly provided detailed description of the GISS-AOM model. We acknowledge the international modeling groups for providing their data for analysis, the Program for Climate Model Diagnosis and Intercomparison (PCMDI) for collecting and archiving the model data, the JSC/CLIVAR Working Group on Coupled Modeling (WGCM) and their Coupled Model Intercomparison Project (CMIP) and Climate Simulation Panel for organizing the model data analysis activity, and the IPCC WG1 TSU for technical support. The IPCC Data Archive at Lawrence Livermore National Laboratory is supported by the Office of Science, U.S. Department of Energy. J. L. Lin was supported by the U.S. CLIVAR CMEP, NOAA CPO/CVP Program, NOAA CPO/CDEP Program, and NASA MAP Program. B. E. Mapes was supported by NSF ATM-0336790K and NOAA OGP CLIVAR-Pacific Program. George Kiladis was supported by NOAA CPO under grant GC05-156.

REFERENCES

AchutaRao, K., and K. R. Sperber, 2006: ENSO Simulation in Coupled Ocean-Atmosphere Models: Are the Current Models Better? *Climate Dyn.*, 10.1007/s00382-006-0119-7.

Adams, D. K., and A. C. Comrie, 1997: The North American monsoon. *Bull. Amer. Meteor. Soc.*, **78**, 2197–2213.

Adler, R.F., G.J. Huffman, A. Chang, R. Ferraro, P. Xie, J. Janowiak, B. Rudolf, U. Schneider, S. Curtis, D. Bolvin, A. Gruber, J. Susskind, and P. Arkin, 2003: The Version 2 Global Precipitation Climatology Project (GPCP) Monthly Precipitation Analysis (1979-Present). J. Hydrometeor., 4,1147-1167.

Anderson B. T., 2002: Regional simulation of intraseasonal variations in the summertime hydrologic cycle over the southwestern United States. *J. Climate*, **15**, 2282–2300.

Anderson B. T., and J. O. Roads, 2002: Regional simulation of summertime precipitation over the southwestern United States. *J. Climate*, **15**, 3321–3342.

Anderson B. T., J. O. Roads, and S.-C. Chen, 2000a: Large-scale forcing of summertime monsoon surges over the Gulf of California and southwestern United States. *J. Geophys. Res*, **105**(D19), 24455–24467.

Anderson B. T., J. O. Roads, S.-C. Chen, and H.-M. H. Juang, 2000b: Regional simulation of the low-level monsoon winds over the Gulf of California and southwestern United States. *J. Geophys. Res*, **105**(D14), 17955–17969.

Anderson B. T., J. O. Roads, and S.-C. Chen, 2001: Model dynamics of summertime low-level jets over northwestern Mexico. *J. Geophys. Res*, **106**(D4), 3401–3413.

Arrit, R. W., D. C. Goering, and C. J. Anderson, 2000: The North American monsoon system in the Hadley Center coupled ocean-atmosphere GCM. Geophy. Res. Let., 27, 565-658.

Avila, L. A., 1991: Eastern North Pacific hurricane season of 1990. *Mon. Wea. Rev.,* **119,** 2034–2046.

Avila, L. A., and R. J. Pasch, 1992: Atlantic tropical systems of 1991. *Mon. Wea. Rev.,* **120,** 2688–2696.

Barlow, M., S. Nigam, and E. H. Berbery, 1998: Evolution of the North American Monsoon System. J. Climate, 11, 2238-2257.

Berbery E. H., and M. S. Fox-Rabinovitz, 2003: Multiscale diagnosis of the North American monsoon system using a variable-resolution GCM. *J. Climate*, **16**, 1929–1947.

Bougeault, P., 1985: A Simple Parameterization of the Large-Scale Effects of Cumulus Convection. *Monthly Weather Review*, 113, 2108–2121.

Capotondi, A., A. Wittenberg, and S. Masina, 2006: Spatial and temporal structure of tropical Pacific interannual variability in 20th century coupled simulations. Ocean Modeling, submitted.

Collier, J. C., and Guang J. Zhang, 2006: Simulation of the North American Monsoon by the NCAR CCM3 and Its Sensitivity to Convection Parameterization. J. Climate, 19, 2851-2866.

Del Genio, A. D., and M.-S. Yao, 1993: Efficient cumulus parameterization for long-term climate studies: The GISS scheme. *The Representation of Cumulus Convection in Numerical Models, Meteor. Monogr.,* No. 46, Amer. Meteor. Soc., 181–184.

Donner, L. J., 1993: A Cumulus Parameterization Including Mass Fluxes, Vertical Momentum Dynamics, and Mesoscale Effects. *Journal of the Atmospheric Sciences*, 50, 889–906.

Douglas, M. W., R. A. Maddox, K. Howard, and S. Reyes, 1993: The Mexican monsoon. *J. Climate*, **6**, 1665–1667.

Duchan, C.E., 1979: Lanczos filtering in one and two dimensions. *J. Appl. Meteor.*, **18**, 1016-1022.

Dunn L. B., and J. D. Horel, 1994a: Prediction of central Arizona convection. Part I: Evaluation of the NGM and Eta Model precipitation forecasts. *Wea. Forecasting*, **9**, 495–507.

Dunn L. B., and J. D. Horel, 1994b: Prediction of central Arizona convection. Part II: Further examination of the Eta Model forecasts. *Wea. Forecasting*, **9**, 508–521.

Emanuel, K. A., 1991: A Scheme for Representing Cumulus Convection in Large-Scale Models. *Journal of the Atmospheric Sciences*, 48, 2313–2329.

Emori, S., T. Nozawa, A. Numaguti and I. Uno (2001): Importance of cumulus parameterization for precipitation simulation over East Asia in June, J. Meteorol. Soc. Japan, 79, 939-947.

Farfán, L. M., and J. A. Zehnder, 1997: Orographic Influence on the Synoptic-Scale Circulations Associated with the Genesis of Hurricane Guillermo (1991). Mon. Wea. Rev., 125, 2683-2698.

Farrara J. D., and J. Yu, 2003: Interannual variations in the southwest U.S. monsoon and sea surface temperature anomalies: A general circulation model study. *J. Climate*, **16**, 1703–1720.

Fuller, R. D., and D. J. Stensrud, 2000: The relationship between tropical easterly waves and surges over the Gulf of California during the North American monsoon. *Mon. Wea. Rev.*, **128**, 2983–2989.

Giorgi F., 1991: Sensitivity of simulated summertime precipitation over the western United States to different physics parameterizations. *Mon. Wea. Rev*, **119**, 2870–2888.

Giorgi F., C. S. Brodeur, and G. T. Bates, 1994: Regional climate change scenarios over the United States produced with a nested regional climate model. *J. Climate*, **7**, 375–399.

Gochis, D. J., W. J. Shuttleworth, and Z.-L. Yang, 2002: Sensitivity of the modeled North American monsoon regional climate to convective parameterization. *Mon. Wea. Rev.*, **130**, 1282–1298.

Gochis, D. J., W. J. Shuttleworth, and Z.-L. Yang, 2003: Hydrometeorological response of the modeled North American monsoon to convective parameterization. *J. Hydrometeor.*, **4**, 235–250.

Gutzler, D. S., H.-K. Kim, R. W. Higgins, H.-M. H. Juang, M. Kanamitsu, K. Mitchell, K. Mo, P. Pegion, E. Ritchie, J.-K. Schemm, S. Schubert, Y. Song, and R. Yang, 2005: The North American Monsoon Model Assessment Project: Integrating Numerical Modeling into a Field-based Process Study. Bulletin of the American Meteorological Society, 86, 1423-1429.

Higgins, R. W., and W. Shi, 2000: Dominant factors responsible for interannual variability of the summer monsoon in the southwestern United States. *J. Climate*, **13**, 759–776.

Higgins, R. W., and W. Shi, 2001: Intercomparison of the principal modes of interannual and intraseasonal variability of the North American Monsoon System. *J. Climate*, **14**, 403–417.

Higgins, R. W., Y. Yao, and X.-L. Wang, 1997: Influence of the North American monsoon system on the U.S. summer precipitation regime. *J. Climate*, **10**, 2600–2622.

Higgins, R. W., NAME Science Working Group, 2003: The North American Monsoon Experiment (NAME). Science and Implementation Plan for NAME, 91 pp. [Available from Climate Prediction Center, 5200 Auth Road, Camp Springs, MD 20746 or online at http://www.joss.ucar.edu/name.].

Higgins, R.W., and coauthors, 2006: The NAME 2004 Field Campaign and Modeling Strategy. Bulletin of the American Meteorological Society, 87, 79-94.

Huffman, G.J., R.F. Adler, M.M. Morrissey, S. Curtis, R. Joyce, B. McGavock, and J. Susskind, 2001: Global precipitation at one-degree daily resolution from multi-satellite observations. *J. Hydrometeor.*, **2**, 36-50.

Janowiak, J. E., and P. A. Arkin, 1991: Rainfall variations in the Tropics during 1986-1989, as estimated from observations of cloud-top temperatures. *J. Geophys. Res.*, **96** (Suppl.), 3359-3373.

Joseph, R., and S. Nigam, 2006: ENSO Evolution and Teleconnections in IPCC's Twentieth-Century Climate Simulations: Realistic Representation? J. Climate, 19, 4360-4377.

George N. Kiladis, Chris D. Thorncroft, and Nicholas M. J. Hall, 2006: Three-Dimensional Structure and Dynamics of African Easterly Waves. Part I: Observations. J. Atmos. Sci., 63, 2212-2230.

Krishnamurti, T. N., D. Bachiochi, Timothy LaRow, Bhaskar Jha, Mukul Tewari, D. R. Chakraborty, Ricardo Correa-Torres, and Darlene Oosterhof, 2000: Coupled Atmosphere–Ocean Modeling of the El Niño of 1997–98. J. Climate, 13,2428-2459.

Kunkel K. E., 2003: Sea surface temperature forcing the upward trend in U.S. extreme precipitation. *J. Geophys. Res.*, **108**, 4020, doi:10.1029/2002/JD002404.

Kanamitsu M., and K. C. Mo, 2003: Dynamical effect of land surface processes on summer precipitation over the southwestern United States. *J. Climate*, **16**, 496–509.

Lau, K.-H., and N.-C. Lau, 1990: Observed Structure and Propagation Characteristics of Tropical Summertime Synoptic Scale Disturbances. Mon. Wea. Rev., 118, 1888-1913.

Li, J., X. Gao, R. A. Maddox, and S. Sorooshian, 2004: Model Study of Evolution and Diurnal Variations of Rainfall in the North American Monsoon during June and July 2002. Mon. Wea. Rev., 132, 2895-2915.

Li, J., X. Gao, R. A. Maddox, and S. Sorooshian, 2005: Sensitivity of North American Monsoon Rainfall to Multisource Sea Surface Temperatures in MM5. Mon. Wea. Rev., 133, 2922-2939.

Liang X., L. Li, K. E. Kunkel, M. Ting, and J. X. L. Wang, 2004: Regional climate model simulation of U.S. precipitation during 1982–2002. Part I: Annual cycle. *J. Climate*, **17**, 3510–3529.

Lin, J. L., 2006: The double-ITCZ problem in IPCC AR4 coupled GCMs: Ocean-atmosphere feedback analysis. *J. Climate*, accepted with minor revisions.

Lin, J. L., and B. E. Mapes, 2004: Radiation budget of the tropical intraseasonal oscillation. *J. Atmos. Sci.*, **61**, 2050-2062.

Lin, J. L., Mapes, B.E., M. Zhang, and M, Newman, 2004: Stratiform precipitation, vertical heating profiles, and the Madden-Julian Oscillation. *J. Atmos. Sci.,* **61**, 296-309.

Lin, J. L., M. H. Zhang, and B. E. Mapes, 2005: Zonal momentum budget of the Madden-Julian Oscillation: The sources and strength of equivalent linear damping. *J. Atmos. Sci.*, **62**, 2172-2188.

Lin, J.L., G.N. Kiladis, B.E. Mapes, K.M. Weickmann, K.R. Sperber, W.Y. Lin, M. Wheeler, S.D. Schubert, A. Del Genio, L.J. Donner, S. Emori, J.-F. Gueremy, F. Hourdin, P.J. Rasch, E. Roeckner, and J.F. Scinocca, 2006: Tropical intraseasonal variability in 14 IPCC AR4 climate models. Part I: Convective signals. *J. Climate*, **19**, 2665-2690.

Lorenz, D. J., and D L. Hartmann, 2006: The Effect of the MJO on the North American Monsoon. J. Climate, 19,333-343.

Madden, R. A., and P. R. Julian, 1994: Observations of the 40-50-day tropical oscillation-A review. *Mon. Wea. Rev.*, **122**, 814-837.

Maloney E. D., and D. L. Hartmann, 2000: Modulation of eastern North Pacific hurricanes by the Madden–Julian oscillation. *J. Climate*, **13**, 1451–1460.

Mo K. C., and H. M. Juang, 2003: Influence of sea surface temperature anomalies in the Gulf of California on North American monsoon rainfall. *J. Geophys. Res.*, **108**, 4112, doi:10.1029/2002JD002403.

Molinari J., D. Knight, M. Dickinson, D. Vollaro, and S. Skubis, 1997: Potential vorticity, easterly waves, and tropical cyclogenesis. *Mon. Wea. Rev.*, **125**, 2699–2708.

Molinari J., D. Vollaro, S. Skubis, and M. Dickinson, 2000: Origins and mechanisms of eastern Pacific tropical cyclogenesis: A case study. *Mon. Wea. Rev.*, **128**, 125–139.

Moorthi, S., and Suarez M. J., 1992: Relaxed Arakawa–Schubert: A parameterization of moist convection for general circulation models. *Mon. Wea. Rev.,* **120**, 978–1002.

Nordeng, T.E., 1994: Extended versions of the convective parameterization scheme at ECMWF and their impact on the mean and transient activity of the model in the tropics. Technical Memorandum No. 206, European Centre for Medium-Range Weather Forecasts, Reading, United Kingdom.

Oort, A. H., and J. J. Yienger, 1996: Observed long-term variability in the Hadley circulation and its connection to ENSO. *J. Climate*, **9**, 2751-2767.

Pan, D.-M., and D. A. Randall (1998), A cumulus parameterization with a prognostic closure, *Q. J. R. Meteorol. Soc*., 124, 949-981.

Petersen, W. A., R. Cifelli, D. J. Boccippio, S. A. Rutledge, and C. Fairall, 2003: Convection and Easterly Wave Structures Observed in the Eastern Pacific Warm Pool during EPIC-2001. J. Atmos. Sci., 60, 1754-1773.

Raymond D. J., C. Lopez-Carillo, and L. L. Cavazos, 1998: Case-studies of developing east Pacific easterly waves. *Quart. J. Roy. Meteor. Soc.*, **124**, 2005–2034.

Russell GL, Miller JR, Rind D, 1995. A coupled atmosphere-ocean model for transient climate change studies. Atmosphere-Ocean 33 (4), 683-730.

Saleeby, S. M., and W. R. Cotton, 2004: Simulations of the North American Monsoon System. Part I: Model Analysis of the 1993 Monsoon Season. J. Climate, 17, 1997-2018.

Schubert, S., R. Dole, H.v.d. Dool, M. Suarez, and D. Waliser, 2002: Proceedings from a workshop on "Prospects for improved forecasts of weather and short-term climate variability on subseasonal (2 week to 2 month) time scales", 16-18 April 2002, Mitchellville, MD, NASA/TM 2002-104606, vol. 23, pp. 171.

Serra Y. L., and R. A. Houze Jr., 2002: Observations of variability on synoptic timescales in the east Pacific ITCZ. *J. Atmos. Sci.*, **59**, 1723–1743.

Slingo, J. M., and Coauthors, 1996: Intraseasonal oscillations in 15 atmospheric general circulation models: Results from an AMIP diagnostic subproject. *Climate Dyn.*, **12**, 325-357.

Stensrud D. J., R. L. Gall, S. L. Mullen, and K. W. Howard, 1995: Model climatology of the Mexican monsoon. *J. Climate*, **8**, 1775–1794.

Tiedke, M., 1989: A comprehensive mass flux scheme for cumulus parameterization in large-scale models. *Mon. Wea. Rev.,* **117**, 1779-1800.

Tokioka, T., K. Yamazaki, A. Kitoh, and T. Ose, 1988: The equatorial 30-60-day oscillation and the Arakawa-Schubert penetrative cumulus parameterization. *J. Meteor. Soc. Japan*, **66**, 883-901.

Vera, C., W. Higgins, J. Amador, T. Ambrizzi, R. Garreaud, D. Gochis, D. Gutzler, D. Lettenmaier, J. Marengo, C. R. Mechoso, J. Nogues-Paegle, P. L. Silva Dias, and C. Zhang, 2006: Toward a Unified View of the American Monsoon Systems. J. Climate, 19, 4977-5000.

Waliser, D., S. Schubert, A. Kumar, K. Weickmann, and R. Dole, 2003b: Proceedings from a workshop on "Modeling, Simulation and Forecasting of Subseasonal Variability", NASA/CP 2003-104606, vol. 25, pp. 62.

Wheeler, M., and G.N. Kiladis, 1999: Convectively Coupled Equatorial Waves: Analysis of Clouds and Temperature in the Wavenumber-Frequency Domain. *J. Atmos. Sci.,* **56**, 374-399.

Xu J., and E. E. Small, 2002: Simulating summertime rainfall variability in the North American monsoon region: The influence of convection and radiation parameterizations. *J. Geophys. Res.*, **107**, 4727, doi:10.1029/2001JD002047.

Xu, J., X. Gaob, J. Shuttleworthc, S. Sorooshiand, and E. Small, 2004: Model Climatology of the North American Monsoon Onset Period during 1980–2001. J. Climate, 17, 3892-3906.

Yang Z.-L., D. Gochis, and W. J. Shuttleworth, 2001: Evaluation of the simulations of the North American monsoon in the NCAR CCM3. *Geophys. Res. Lett.*, **28**, 1211–1214.

Zehnder J., D. M. Powell, and D. L. Ropp, 1999: The interaction of easterly waves, orography, and the intertropical convergence zone in the genesis of eastern Pacific tropical cyclones. *Mon. Wea. Rev.*, **127**, 1566–1585.

Zhang G. J., and N. A. McFarlane, 1995: Sensitivity of climate simulations to the parameterization of cumulus convection in the Canadian Climate Centre general circulation model. *Atmos.–Ocean*, **33**, 407–446.

FIGURE CAPTIONS

Figure 1. Schematic depiction of the North American monsoon and its two dominant intraseasonal modes: MJO and easterly waves.

Figure 2. Seasonal variation of precipitation averaged over (a) the core region of North American monsoon between 20N-32.5N and 245E-260E, and (b) the eastern Pacific warm pool region between 10N-20N and 245E-260E.

Figure 3. Seasonal variation of precipitation averaged between 245E and 260E for observation and 22 models.

Figure 4. July mean precipitation for observation (GPCP) and 22 IPCC AR4 coupled GCMs.

Figure 5. Variance of the MJO averaged between 5N and 25N.

Figure 6. Ratio between the variance of the MJO and the variance of its westward counterpart (westward wavenumbers 1-6, 24-70 day mode). The variances are averaged over an eastern Pacific box between 5N-25N and 220E-260E.

Figure 7. Lag-correlation of the 24-70 day precipitation anomaly averaged between 5N-25N with respect to itself at 15N245E. Shading denotes the regions where lag-correlation is above the 95% confidence level. The three thick lines correspond to phase speed of 3, 5, and 8 m/s, respectively.

Figure 8. Variance of easterly waves averaged between 10N and 20N.

Figure 9. Ratio between the variance of the westward-propagating easterly waves and the variance of its eastward-propagating counterpart (eastward 3-6 day mode). The variances are averaged over 10N-20N and 240E-290E.

Table 1 List of models that participate in this study

Modeling Groups	IPCC ID (Label in Figures)	Grid type/ Resolution/ Model top	Deep convection scheme / Modification	Downdrafts[2] SC/UC/Meso	Closure/ Trigger	Flux correction
National Center for Atmospheric Research	CCSM3 (CCSM3)	Spectral T85*L26 2.2mb	Zhang and McFarlane (1995)	Y/N/N	CAPE	N
National Center for Atmospheric Research	PCM (PCM)	Spectral T42*L26 2.2mb	Zhang and McFarlane (1995)	Y/N/N	CAPE	N
Canadian Centre for Climate Modeling & Analysis	CGCM3.1-T47 (CGCM-T47)	Spectral T47*L32 1mb	Zhang & McFarlane (1995)	Y/N/N	CAPE	Heat, water
Canadian Centre for Climate Modeling & Analysis	CGCM3.1-T63 (CGCM-T63)	Spectral T63*L32 1mb	Zhang & McFarlane (1995)	Y/N/N	CAPE	Heat, water
LASG/Institute of Atmospheric Physics	FGOALS-g1.0 (IAP)	Gridpoint 64*32*L32 2mb	Zhang & McFarlane (1995)	Y/N/N	CAPE	N
NASA/ Goddard Institute for Space Studies	GISS-AOM (GISS-AOM)	Gridpoint 90*60*L12	Russell et al. (1995)	N/N/N	CAPE	N
NASA/ Goddard Institute for Space Studies	GISS-ER (GISS-ER)	Gridpoint 72*46*L20 0.1mb	Del Genio and Yao (1993)	Y/N/N	Cloud base buoyancy	N
NASA/ Goddard Institute for Space Studies	GISS-EH (GISS-EH)	Gridpoint 72*46*L20 0.1mb	Del Genio and Yao (1993)	Y/N/N	Cloud base buoyancy	N
Hadley Centre for Climate Prediction and Research / Met Office	UKMO-HadCM3 (HadCM3)	Spectral T63*L18 4mb	Gregory and Rowntree (1990)	Y/N/N	Cloud base buoyancy	N
Hadley Centre for Climate Prediction and Research / Met Office	UKMO-HadGEM1 (HadGEM1)	Spectral T63*L18 4mb	Gregory and Rowntree (1990)	Y/N/N	Cloud base buoyancy	N
CSIRO Atmospheric Research	CSIRO Mk3.0 (CSIRO)	Spectral T63*L18 4mb	Gregory and Rowntree (1990)	Y/N/N	Cloud base buoyancy	N
Meteorological Research Institute	MRI-CGCM2.3.2 (MRI)	Spectral T42*L30 0.4mb	Pan and Randall (1998)	Y/N/N	CAPE	Heat, water
Center for Climate System Research (The University of Tokyo), National Institute for Environmental Studies, and Frontier Research Center for Global Change	MIROC3.2–hires (MIROC-hires)	Spectral T106*L56	Pan and Randall (1998) / Emori et al. (2001)	Y/N/N	CAPE/ Relative humidity	N
Same as above	MIROC3.2-medres (MIROC-medres)	Spectral T42*L20 30 km	Pan and Randall (1998) / Emori et al. (2001)	Y/N/N	CAPE/ Relative humidity	N

NOAA / Geophysical Fluid Dynamics Laboratory	GFDL-CM2.0 (GFDL2.0)	Gridpoint 144*90*L24 3mb	Moorthi and Suarez (1992) / Tokioka et al. (1988)	N/N/N	CAPE/ Threshold	N
NOAA/ Geophysical Fluid Dynamics Laboratory	GFDL-CM2.1 (GFDL2.1)	Gridpoint 144*90*L24 3mb	Moorthi and Suarez (1992) / Tokioka et al. (1988)	N/N/N	CAPE/ Threshold	N
Max Planck Institute for Meteorology	ECHAM5/ MPI-OM (MPI)	Spectral T63*L31 10mb	Tiedtke (1989) / Nordeng (1994)	Y/N/N	CAPE/ Moisture convergence	N
Meteorological Institute of the University of Bonn, Meteorological Research Institute of KMA, and Model and Data Group	ECHO-G (ECHO-G)	Spectral T30*L19 10mb	Tiedtke (1989) / Nordeng (1994)	Y/N/N	CAPE/ Moisture convergence	Heat, water
Mateo-France / Centre National de Recherches Météorologiques	CNRM-CM3 (CNRM)	Spectral T63*L45 0.05mb	Bougeault (1985)	N/N/N	Kuo	N
Bjerknes Centre for Climate Research	BCCR-BCM2.0 (BCCR)	Spectral T63*L31 10mb	Bougeault (1985)	N/N/N	Kuo	N
Institute for Numerical Mathematics	INM-CM3.0 (INM)	Gridpoint 72*45*L21	Betts (1986)	N/N/N	CAPE	Water
Institute Pierre Simon Laplace	IPSL-CM4 (IPSL)	Gridpoint 96*72*L19	Emanuel (1991)	Y/Y/N	CAPE	N

* For downdrafts, SC means saturated convective downdrafts, UC means unsaturated convective downdrafts, and Meso means mesoscale downdrafts.

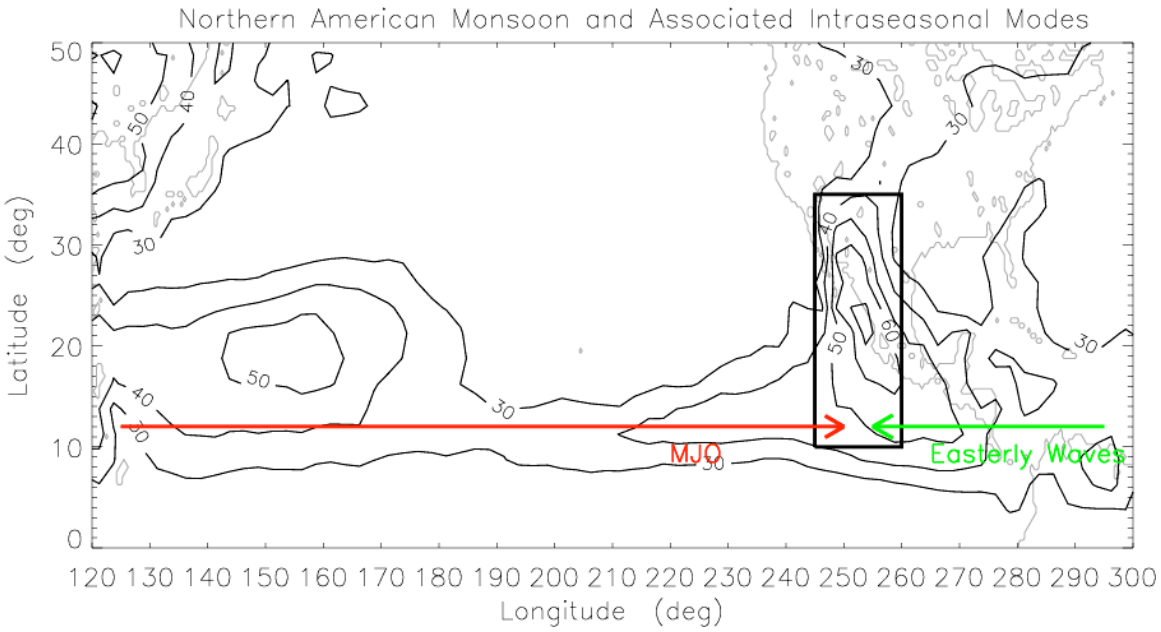

Figure 1. Schematic depiction of the North American monsoon and its two dominant intraseasonal modes: MJO and easterly waves. Contour denotes the percentage of annual mean GPCP precipitation that falls in the monsoon season (July to September). The box denotes the monsoon region.

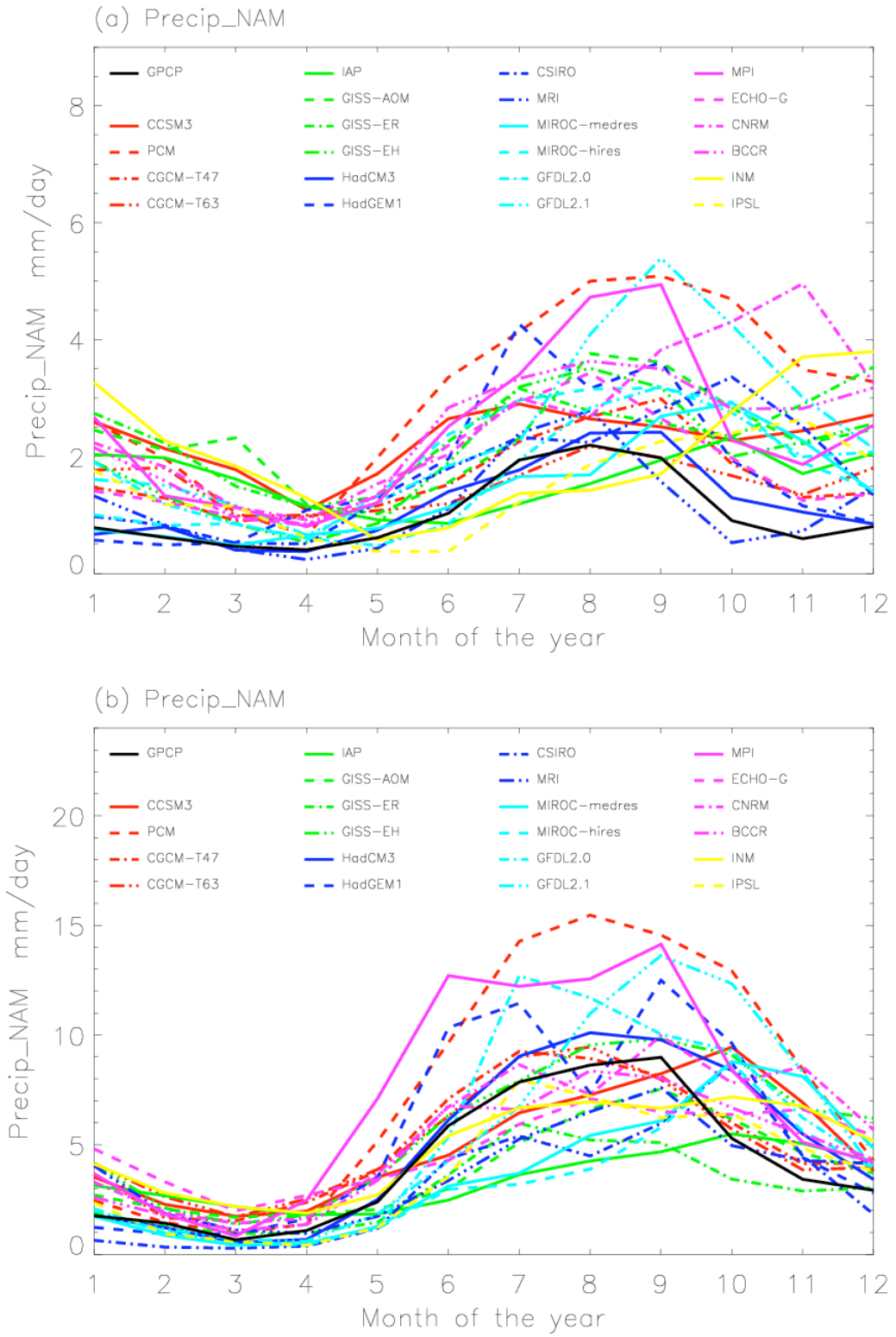

Figure 2. Seasonal variation of precipitation averaged over (a) the core region of North American monsoon between 20N-32.5N and 245E-260E, and (b) the eastern Pacific warm pool region between 10N-20N and 245E-260E.

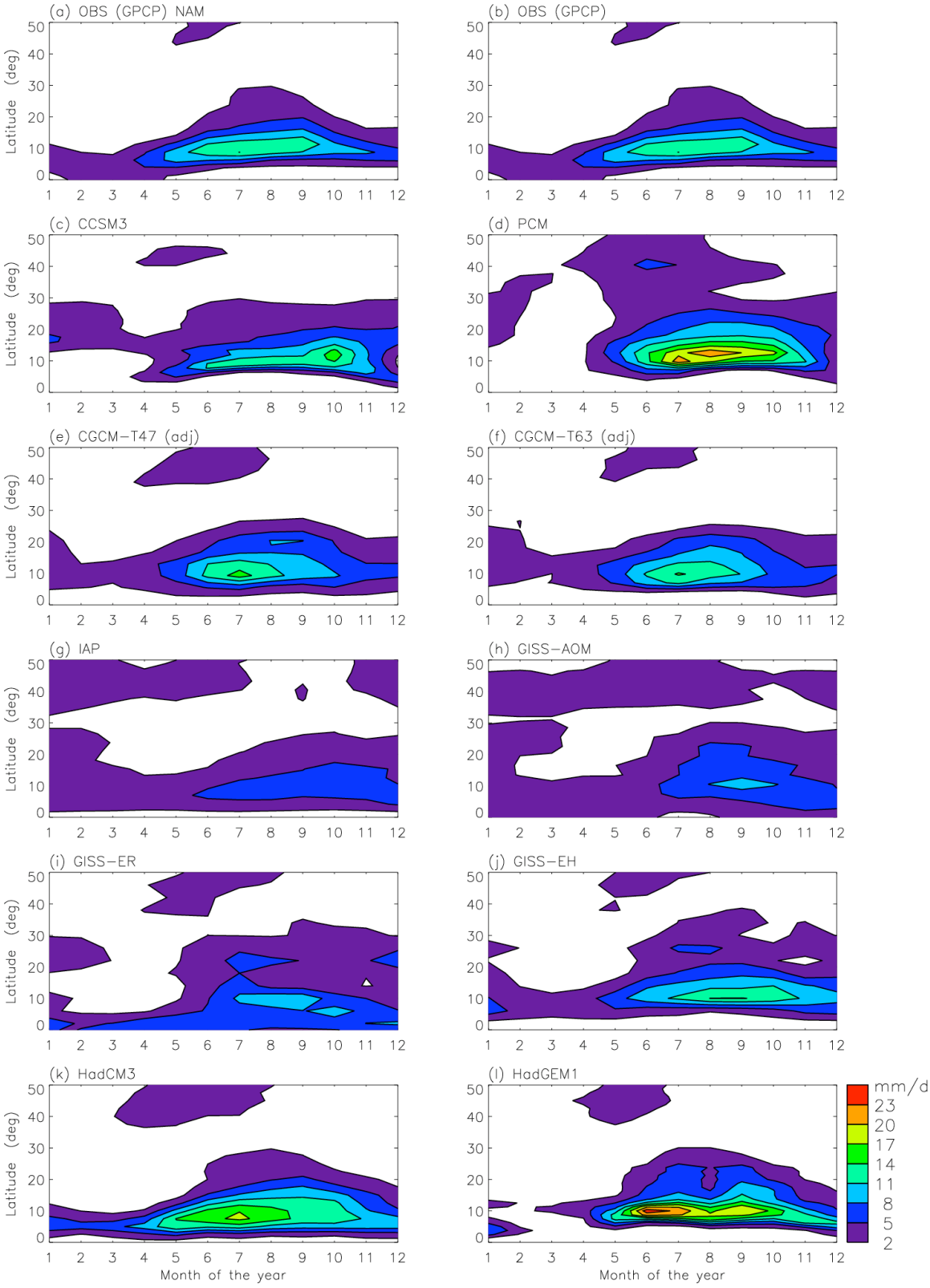

Figure 3. Seasonal variation of precipitation averaged between 245E and 260E for observation and 22 models.

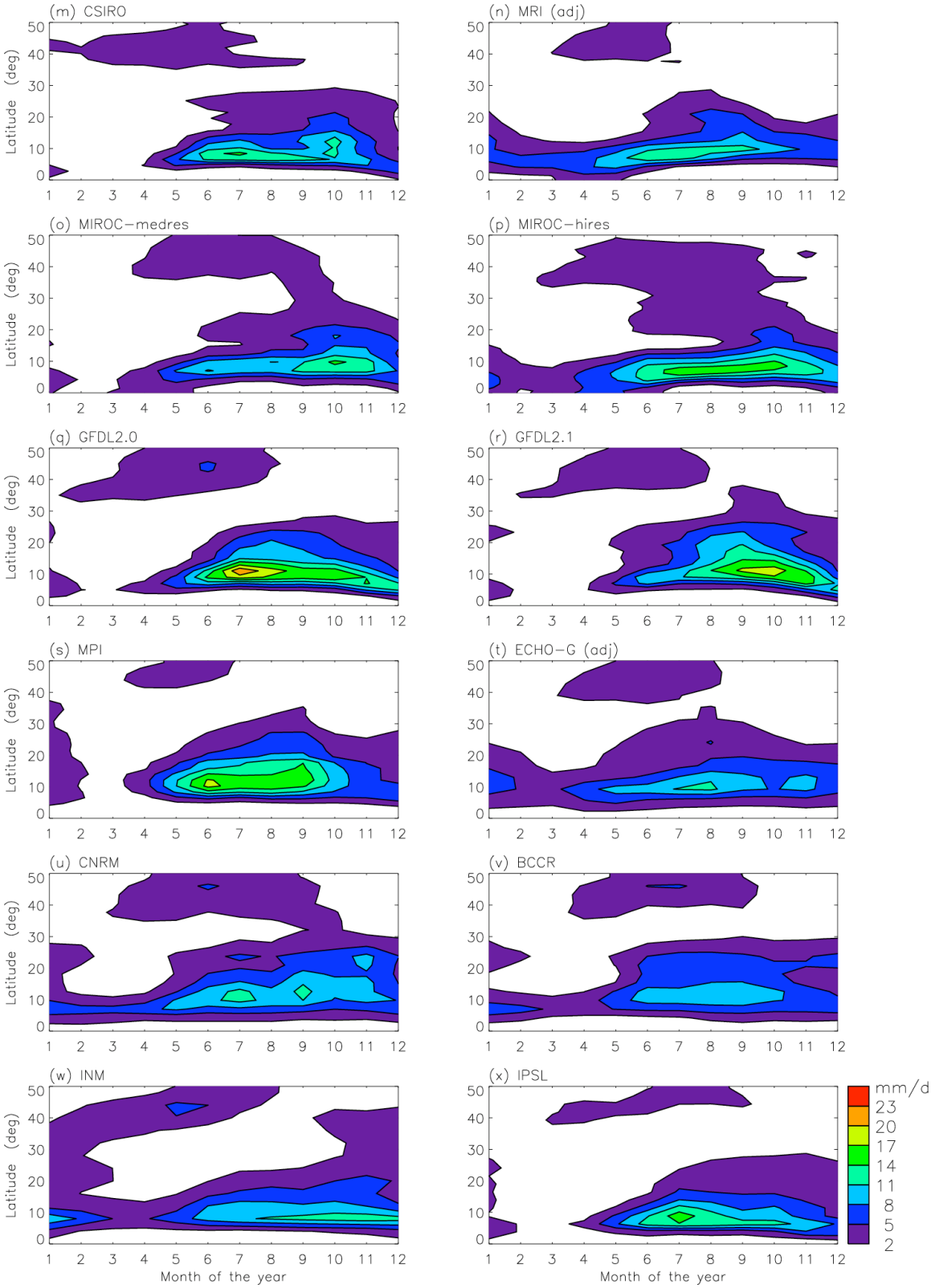

Figure 3. Continued.

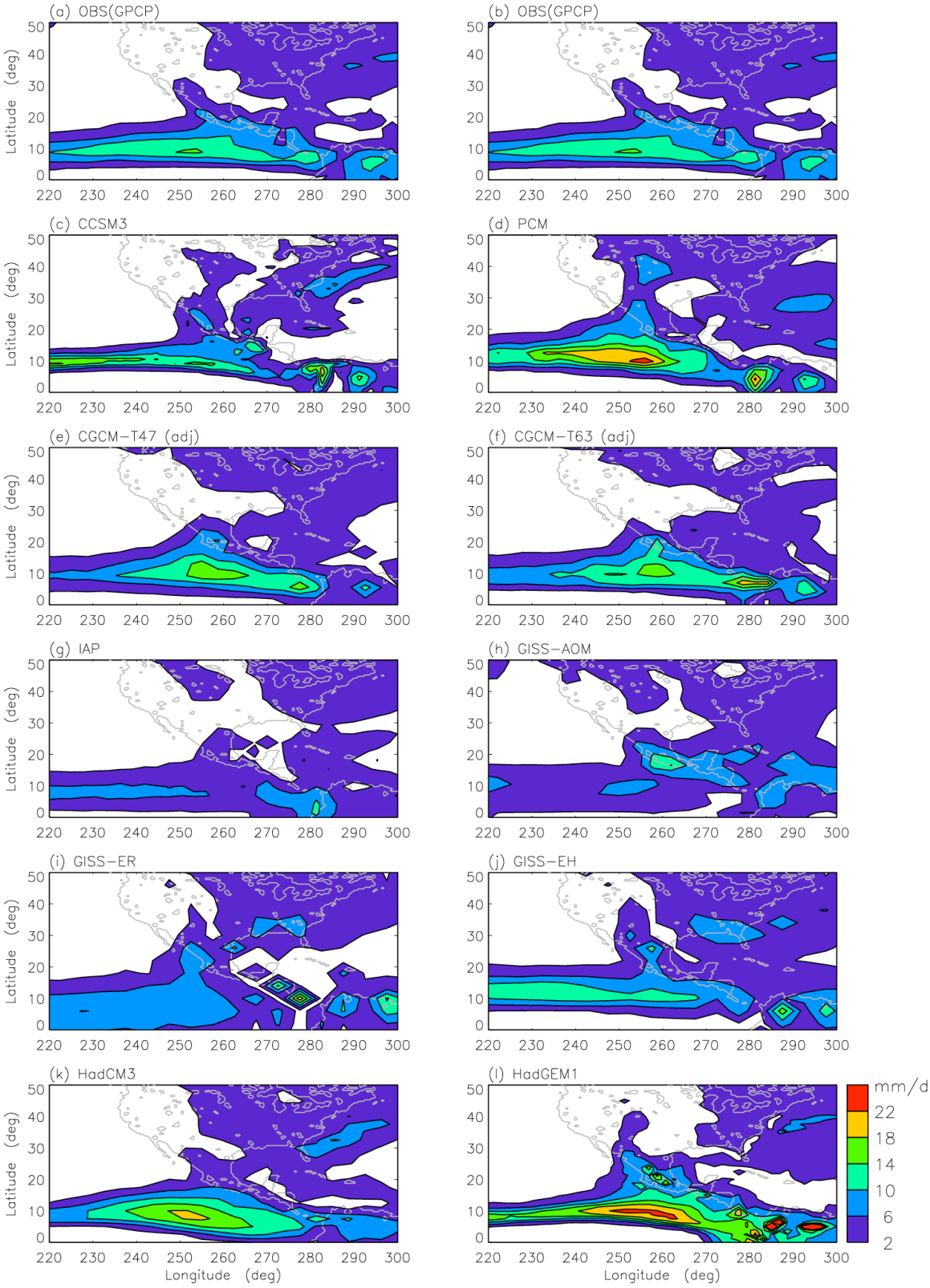

Figure 4. July mean precipitation for observation (GPCP) and 22 IPCC AR4 coupled GCMs.

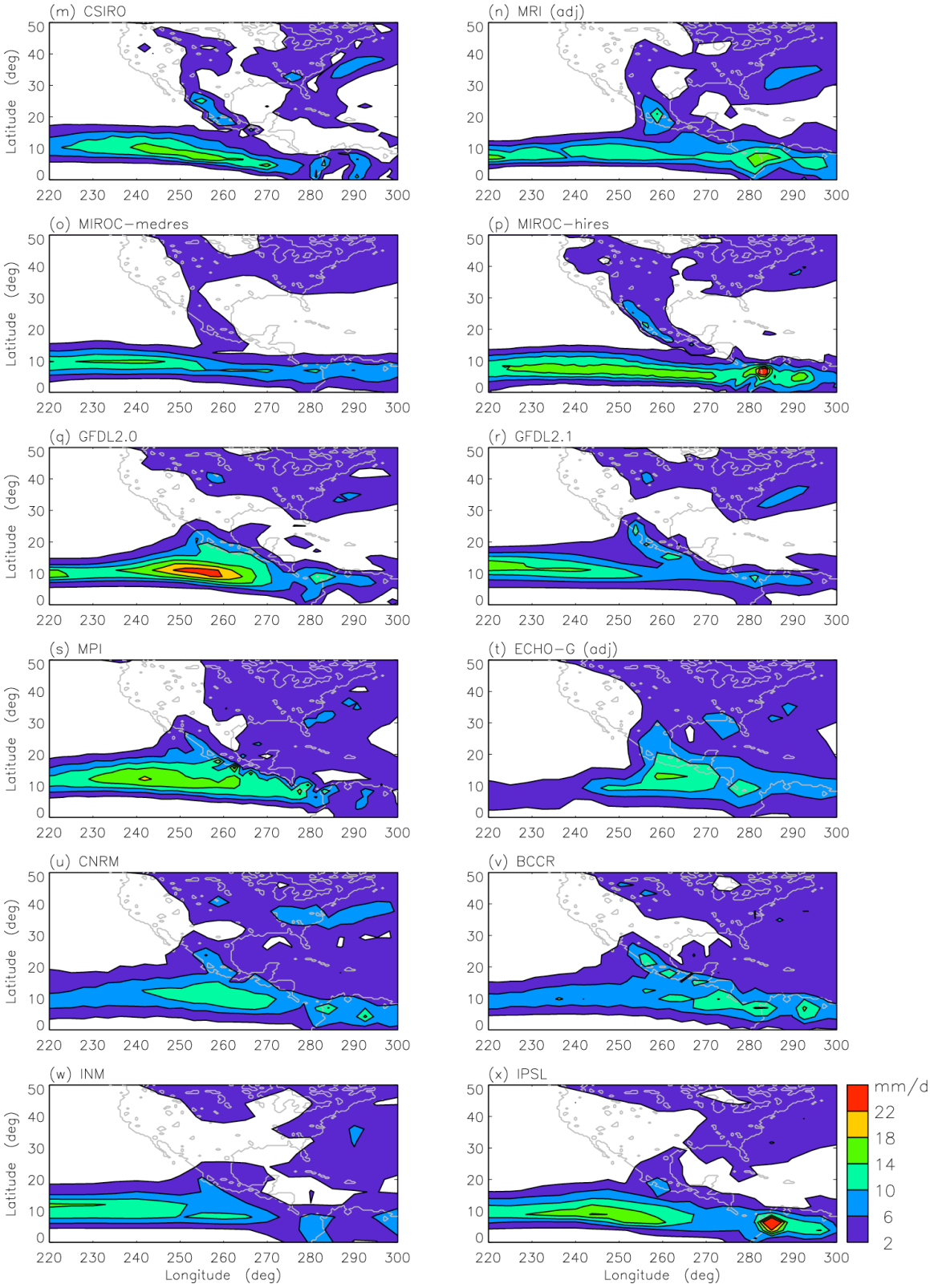

Figure 4. Continued.

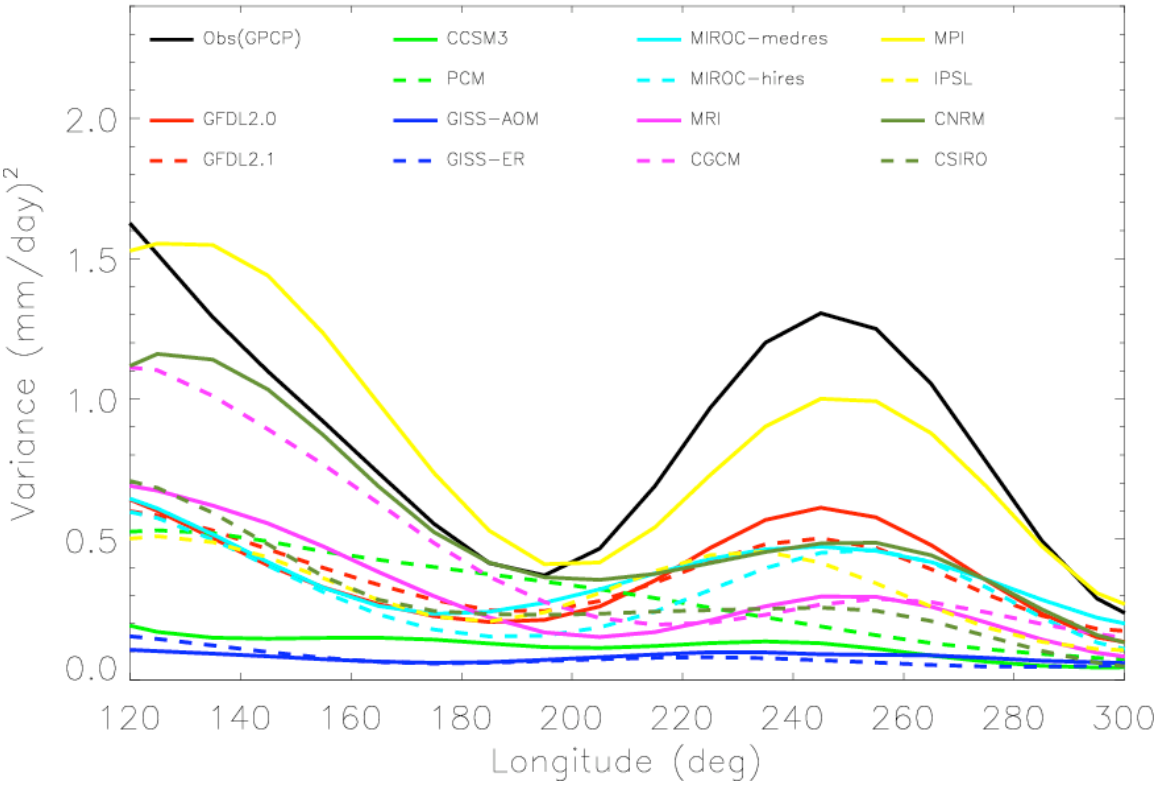

Figure 5. Variance of the MJO averaged between 5N and 25N.

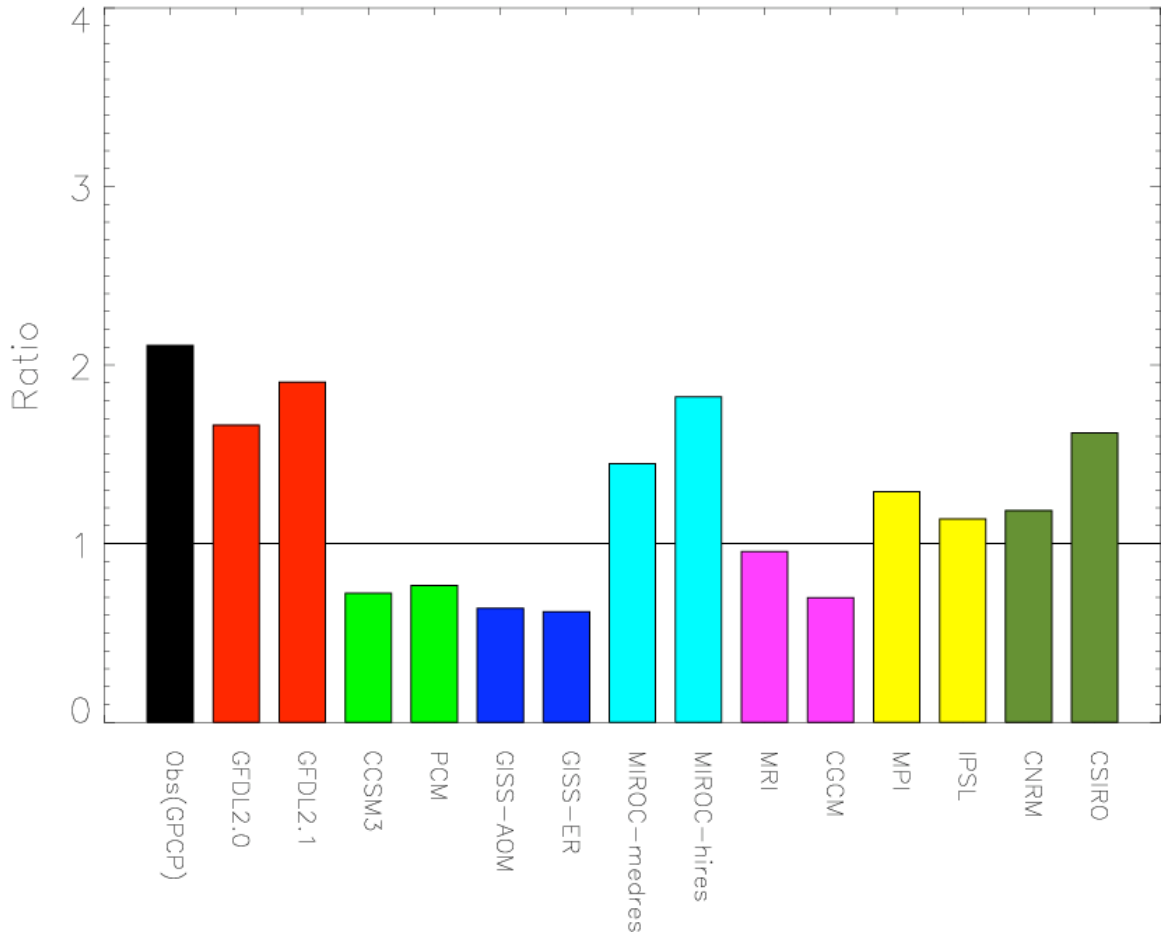

Figure 6. Ratio between the variance of the MJO and the variance of its westward counterpart (westward wavenumbers 1-6, 24-70 day mode). The variances are averaged over an eastern Pacific box between 5N-25N and 220E-260E.

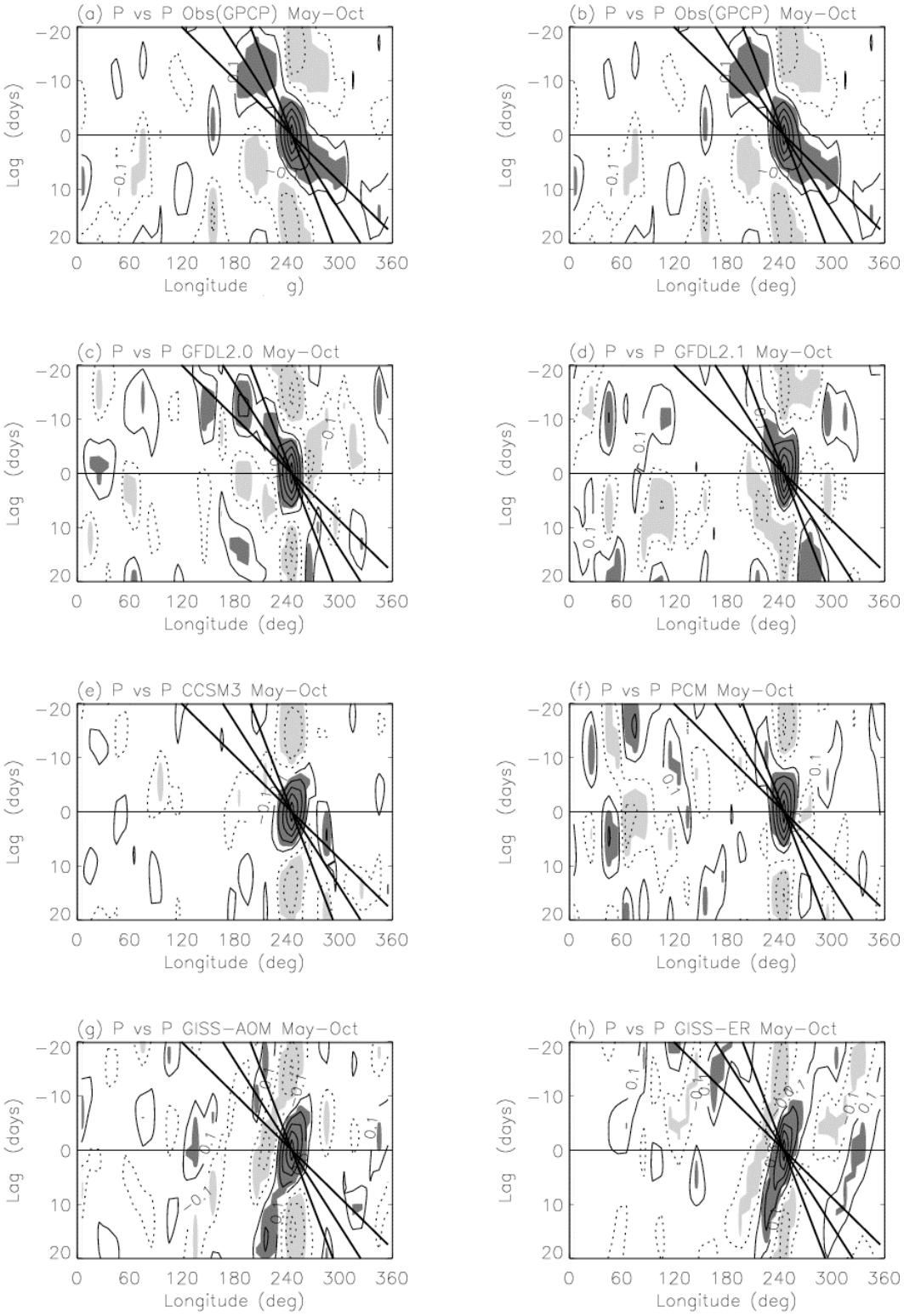

Figure 7. Lag-correlation of the 24-70 day precipitation anomaly averaged between 5N-25N with respect to itself at 15N245E. Shading denotes the regions where lag-correlation is above the 95% confidence level. The three thick lines correspond to phase speed of 3, 5, and 8 m/s, respectively.

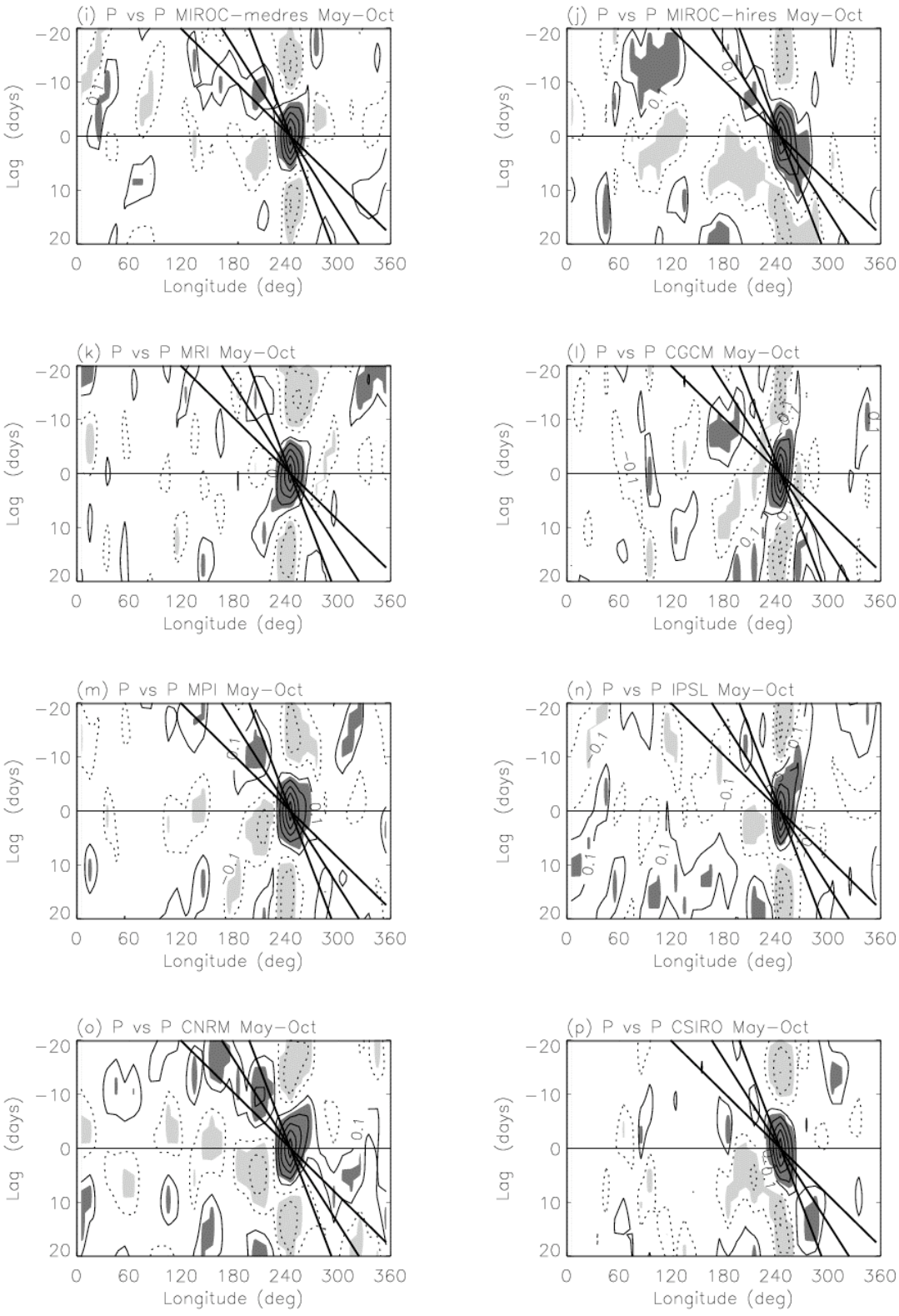

Figure 7. Continued.

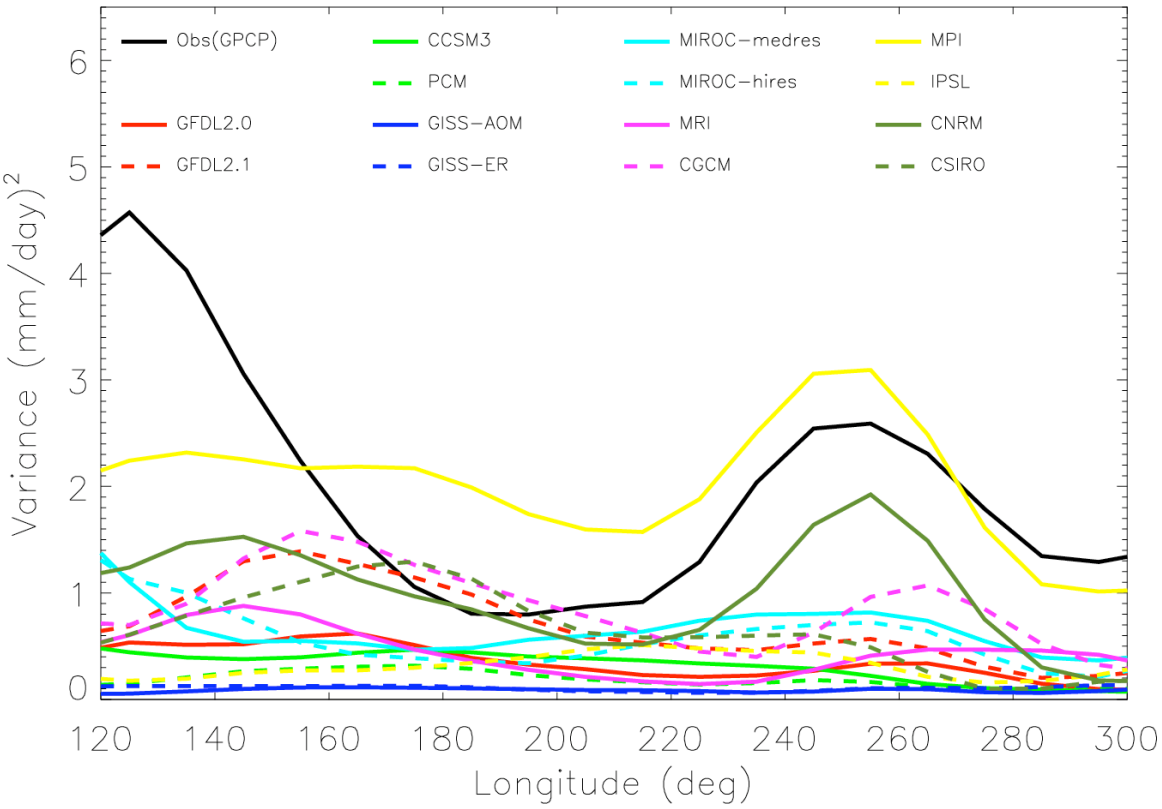

Figure 8. Variance of easterly waves averaged between 10N and 20N.

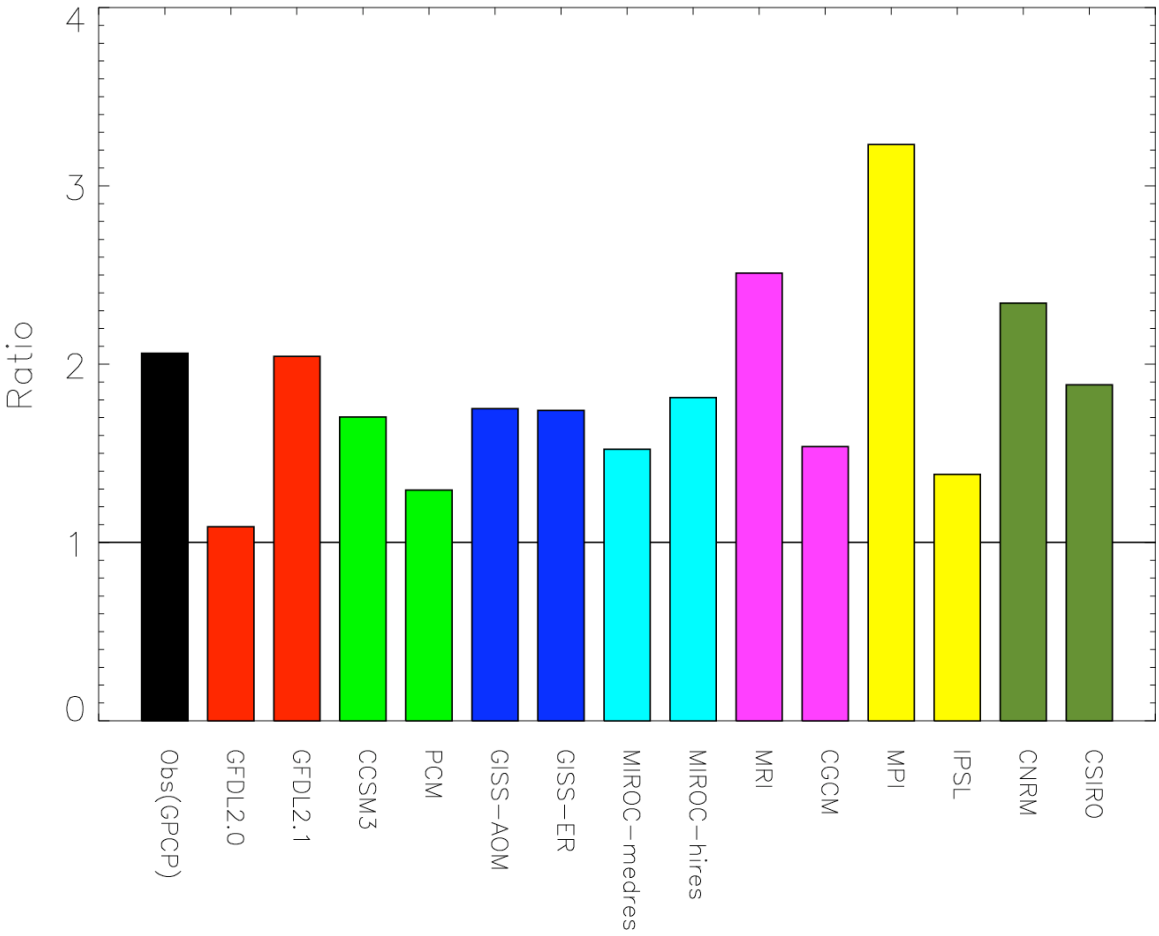

Figure 9. Ratio between the variance of the westward-propagating easterly waves and the variance of its eastward-propagating counterpart (eastward 3-6 day mode). The variances are averaged over 10N-20N and 240E-290E.